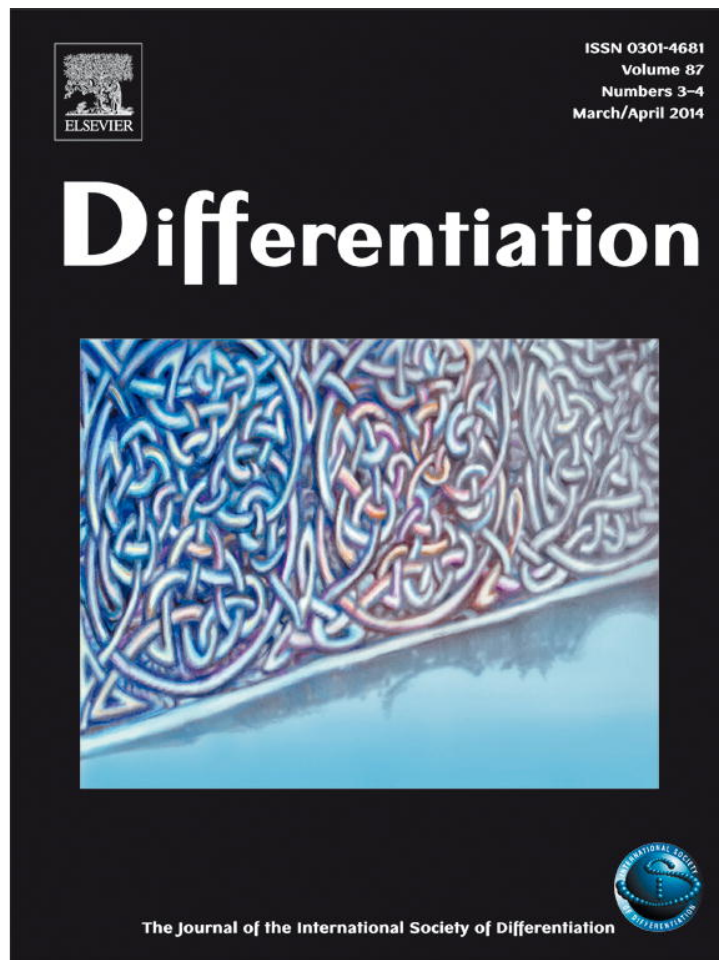


Provided for non-commercial research and education use.
Not for reproduction, distribution or commercial use.



This article appeared in a journal published by Elsevier. The attached copy is furnished to the author for internal non-commercial research and education use, including for instruction at the authors institution and sharing with colleagues.

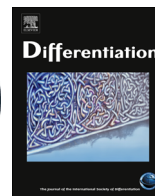
Other uses, including reproduction and distribution, or selling or licensing copies, or posting to personal, institutional or third party websites are prohibited.

In most cases authors are permitted to post their version of the article (e.g. in Word or Tex form) to their personal website or institutional repository. Authors requiring further information regarding Elsevier's archiving and manuscript policies are encouraged to visit:

<http://www.elsevier.com/authorsrights>

Contents lists available at [ScienceDirect](http://www.sciencedirect.com)

Differentiation

journal homepage: www.elsevier.com/locate/diff

c-Kit identifies a subpopulation of mesenchymal stem cells in adipose tissue with higher telomerase expression and differentiation potential



A. Blazquez-Martinez^a, M. Chiesa^a, F. Arnalich^b, J. Fernandez-Delgado^c,
M. Nistal^d, M.P. De Miguel^{a,*}

^a Cell Engineering Laboratory, La Paz University Hospital Research Institute, Madrid, Spain

^b Department of Internal Medicine, La Paz University Hospital, Madrid, Spain

^c Department of Plastic and Reconstructive Surgery, Santa Cristina Hospital, and Centrocim, Madrid, Spain

^d Department of Pathology, La Paz University Hospital, Madrid, Spain

ARTICLE INFO

Article history:

Received 26 April 2013

Received in revised form

24 January 2014

Accepted 24 February 2014

Available online 6 April 2014

Keywords:

Adipose-derived stem cells

c-Kit

Pluripotency

Differentiation

Self-renewal

Telomerase

ABSTRACT

The stromal vascular fraction (SVF) of adipose tissue is an easy to obtain source of adipose tissue-derived stem cells (ADSCs). We and others have achieved significant but suboptimal therapeutic effects with ADSCs in various settings, mainly due to low rates of differentiation into specific cell types and with the downside of undesired side effects as a consequence of the undifferentiated ADSCs. These data prompted us to find new stem cell-specific markers for ADSCs and/or subpopulations with higher differentiation potential to specific lineages. We found a subpopulation of human ADSCs, marked by c-Kit positiveness, resides in a perivascular location, and shows higher proliferative activity and self-renewal capacity, higher telomerase activity and expression, higher in vitro adipogenic efficiency, a higher capacity for the maintenance of cardiac progenitors, and higher pancreatogenic and hepatogenic efficiency independently of CD105 expression. Our data suggests that the isolation of ADSC subpopulations with anti-c-Kit antibodies allows for the selection of a more homogeneous subpopulation with increased cardioprotective properties and increased adipogenic and endodermal differentiation potential, providing a useful tool for specific therapies in regenerative medicine applications.

© 2014 International Society of Differentiation. Published by Elsevier B.V. All rights reserved.

1. Introduction

Mesenchymal stem cells (MSCs) have been found in a variety of adult tissues, such as bone marrow, trabecular bone (Nöth et al., 2002; Tuli et al., 2003), skin (Toma et al., 2005), blood vessels (Sampaolesi et al., 2003), muscle and brain (Jiang et al., 2002), synovium (De Bari et al., 2001), skeletal muscle (Jankowski et al., 2002), lung (Noort et al., 2002), decidua teeth (Miura et al., 2003) and adipose tissue (Zuk et al., 2001; Gronthos et al., 2001; De Ugarte et al., 2003).

The stromal vascular fraction (SVF) of adipose tissue is an easy to obtain source of adipose tissue-derived mesenchymal stem cells (ADSCs). Relatively recent studies suggest that the MSCs in this stroma are similar to bone marrow MSCs (Zuk et al., 2001; Gronthos et al., 2001; De Ugarte et al., 2003). A minimum of three

criteria has been established as necessary to consider a cell population as MSCs (Dominici et al., 2006). First, MSCs must be plastic-adherent when maintained in standard culture conditions. Second, MSCs must express CD105, CD73 and CD90 and lack expression of CD45, CD34, CD14 or CD11b, CD79α or CD19 and HLA-DR surface molecules. Third, MSCs must have the ability to differentiate to the adipogenic, chondrogenic and osteogenic mesodermal lineages.

The establishment of CD105 as a stem cell marker in adipose-derived tissue was based on its bone marrow counterparts (Lee et al., 2004; Sengenès et al., 2005; Boquest et al., 2005). Interestingly, more than 90% of adherent cells from unsorted SVFs acquire CD105 when cultured (Yoshimura et al., 2006; Varma et al., 2007). Subsequently, whole cultured SVF has been used for therapeutic purposes in most published studies. However, no correlation between CD105 positiveness and true stemness markers has been reported (Park and Patel, 2010; Wan Safwani et al., 2011).

ADSCs have been shown to have the potential to differentiate preferentially and with high efficiency into mesodermal cells, such as adipocytes, fibroblasts, myocytes, osteocytes and chondrocytes,

* Correspondence to: Cell Engineering Laboratory, La Paz University Hospital Research Institute, IDiPAZ, Paseo Castellana 261, Madrid 28046 Spain.
Tel.: +34 91 2071458; fax: +34 91 7277050.

E-mail address: mariapdemiguel@gmail.com (M.P. De Miguel).

<http://dx.doi.org/10.1016/j.diff.2014.02.007>

Join the International Society for Differentiation (www.isdifferentiation.org)

0301-4681/© 2014 International Society of Differentiation. Published by Elsevier B.V. All rights reserved.

in a process known as lineage-specific differentiation (Mizuno et al., 2002; Gimble and Guilak, 2003; Ogawa et al., 2004). In addition, there is increasing evidence of the ability of ADSCs to differentiate into non-mesodermal cells (Schäffler et al., 2007), such as endothelial cells (Wosnitza et al., 2007), cardiomyocytes (Bai et al., 2007), neurons (Ning et al., 2006), hepatocytes (Seo et al., 2005) and pancreatic cells (Timper et al., 2006) from adequately stimulated ADSCs in vitro, although at lower efficiencies.

We and others have achieved significant but suboptimal therapeutic effects with ADSCs in various settings, mainly due to the low rates of differentiation into specific cell types, and with the downside of undesired side effects as a consequence of the undifferentiated ADSCs: For example, a high proarrhythmic risk has been described for myocardial infarction, suggesting that adult stem cells fail to electromechanically integrate within the recipient's heart, thereby mandating the search for second-generation cell types able to achieve this goal, which is the prerequisite for an effective enhancement of contractile function (Menasché, 2005). In another setting, we injected ADSCs in a rabbit model of stromal corneal damage. The ADSCs achieved differentiation into stromal corneal keratocytes; however, only in a small percentage, resulting in suboptimal transparency and corneal regeneration (Arnalich-Montiel et al., 2008).

Several authors have identified ADSC subpopulations with higher mesodermal differentiation potential: Varma et al. (2007) identified that freshly isolated ADSC were CD34 and c-Kit positive and displayed higher osteogenic potential in vitro than cultured ADSCs. Stro1+ cells show higher osteogenic potential and CD105+CD29+ higher chondrogenic potential (Rada et al., 2011). A L-NGFR+ isolated subpopulation showed increased adipogenic, chondrogenic and osteogenic potential (Quirici et al., 2010).

These data prompted us to search for new stem cell-specific markers for ADSCs and/or subpopulations with higher differentiation potential to specific lineages in order to improve the differentiation efficiency and thus the therapeutic effect and lower side effects of in vivo therapies using ADSCs.

2. Material and methods

2.1. Isolation of stromal vascular fraction (SVF) from human and mouse adipose tissue

SVF was prepared from a total of 16 samples (300 ml each) of lipoaspirated adipose tissue from 16 separate human donors undergoing elective liposuction after giving their informed consent. Age from 16 patients used ranged from 25 to 55 years old, mean 38.75 y.o. All patients were female, with BMI ranging from 26.3 to 29.3, mean 27.5. The isolation protocols were approved by the Institutional Review Boards of La Paz Hospital (Madrid, Spain) and were in accordance with the Declaration of Helsinki (2000) of the World Medical Association. In addition, adipose tissue from the inguinal-peritoneal region of Swiss mice was processed. All mouse protocols were approved by the La Paz Hospital Animal Welfare Committee.

Isolation process was previously described (Hauner et al., 1987; Katz et al., 1999). Briefly, after washing with PBS (Gibco-BRL, Grand Island, NY, USA), each sample was digested with collagenase I (0.075% in PBS, from Gibco) for 30' at 37 °C under gentle agitation (for mouse 0.09% collagenase was used). Upon centrifugation (300g, 10', RT), the pellet was resuspended in erythrocyte lysis buffer (160 mM NH₄Cl, 10 mM KHCO₃, 1 mM EDTA, all from Sigma) for 10' at RT. The SVF was then recollected by centrifugation (300g 10', RT) and seeded in 10-cm diameter culture plates (Corning, Corning, NY, USA) at a density of 3×10^4 cells/cm² and cultivated in DMEM (Gibco) supplemented with 10% FBS (Gibco) and 1% Pen/Strep (Sigma).

2.2. Clonogenic cell culture

To obtain cellular clones of hADSCs, SVF cells were isolated by serial dilution and plated in 384-well Terasaki multiwell-plates (BD Falcon, Franklin Lakes, NJ, USA) at 1 cell per well, and passaged as needed into larger wells until reaching subconfluence in a 10 cm plate.

2.3. Extraction of mice embryo cardiomyocytes

The myocardia of 14.5-day post-coitum mouse embryos was digested with 0.1% collagenase I and 0.025% Trypsin-EDTA for 5' at 37 °C. Upon extensive pipetting, the reaction was inhibited by the addition of an equal volume of DMEM, 10% FBS, 5% Horse Serum (Gibco), 1% Pen/Strep and 0.1% Fungizone (Gibco) before seeding in the same medium.

2.4. Mice perfusion

Mice were anesthetized by an injection of Ketolar (0.01 ml/10 g mouse weight) and Domtor (0.005 ml/10 g mouse weight, both from Pfizer, NY, USA). A cannula was then inserted in the right heart ventricle to pump PBS, and the blood was drained through an incision in the left heart atrium. Once the mouse was completely bled out, the inguinal adipose tissue was extracted.

2.5. Immunohistochemistry

Human adipose tissue samples were fixed for 24 h in 3.7% formaldehyde and then paraffin-embedded. Five-micrometer sections were incubated with primaries antibodies (anti-human c-Kit, 1:100, and anti-CD31, 1:200, both from Dako) for 1 h and then incubated with biotin-conjugated secondary antibodies (1:100, Vector Labs, Burlingame, CA, USA) for 30'. Samples were then incubated with avidin-peroxidase complex, stained with DAB and avidin-alkaline phosphatase, stained with Fast Red (all from Vector) and counterstained with Harris Hematoxylin (Dako).

2.6. Immunocytochemistry

Fixed (4% paraformaldehyde, PFA) cultured samples were previously washed with 1 M citric acid or 3% H₂O₂ to inhibit the endogenous alkaline phosphatase or peroxidase, respectively. After blocking and permeabilizing with PBS 0.1% Tween-20 (Sigma) and 10% FBS or goat serum, the samples were incubated with the following primary antibodies at the indicated concentration: anti-sarcomeric actin, anti-insulin, anti-albumin (1:50, all from Dako), anti-GATA4 (1:100, Novus Biologicals), anti-c-Kit (1:200, Dako), anti-human troponin (1:50, Sigma Prestige). Samples were incubated with the proper biotin-conjugated secondary antibody (1:100, Vector Labs, Burlingame, CA, USA) for 30'. After incubation with avidin-peroxidase complex or avidin alkaline phosphatase, the samples were stained with either DAB (Vector) or 1% Naphthol AS-MX (Sigma) and Fast Red-TR (1 mg/ml, Sigma). When required, the samples were counterstained with Harris, Cole's (Dako) or Mayer's (handmade) hematoxylin. For immunofluorescence, the samples were incubated with PBS 0.1% Tween-20, 3% goat serum and 1% BSA containing the following secondary antibodies: Texas Red conjugated anti-mouse, fluorescein conjugated anti-mouse or anti-rabbit (1:100, all from Vector), or rhodamine conjugated anti-rabbit (1:50, Boehringer Ingelheim GmbH, DL). Samples were then mounted with DAPI-containing Vectashield (Vector Labs).

2.7. Flow cytometry and cell sorting

Cells were resuspended in PBS 15% FBS and incubated for 20' at 4 °C with the following antibodies: phycoerythrin-conjugated anti-c-Kit, fluorescein-conjugated anti-CD24, (all from Becton Dickinson) and fluorescein-conjugated anti-CD105 (Chemicon). Cells were then resuspended in PBS 1% BSA and analyzed in a cytometer (BD, Franklin Lakes, NJ, USA) using the Cell Quest Pro program. For the mouse cells, the antibody anti-c-Kit (eBiosciences, clone ACK2) was used once conjugation had been achieved with the secondary anti-mouse TRICT (Sigma). To isolate the human cellular fractions based on c-Kit and/or CD105 expression, the cells were analyzed in a cytometer with a cell separation module (MoFlo, Dako).

2.8. Magnetic cell separation

SVF cells were selected by magnetic separation by anti-c-Kit and anti-CD105 antibodies conjugated MicroBeads (Miltenyi Biotec Inc., Auburn CA, USA), used according to the manufacturer's instructions, and used directly for the differentiation protocols without further expansion.

2.9. Proliferation rate analysis

Cells at different time points were incubated for 24 h with BrdU before fixing and stained according to the manufacturers' protocol (Amersham). Five hundred nuclei were counted as positive or negative, and the data were statistically analyzed with the Mann-Whitney *U* test.

2.10. Chondrogenesis

hADSCs were plated using the micromass culturing technique (Im et al., 2005). A 10 µl culture media drop containing 8×10^6 cells/ml suspension was plated in normal medium. Five hours later, the culture media was replaced by a chondrogenic differentiation culture media: DMEM, ITS 1 × (Sigma), 0.1 µM dexamethasone (Merk, Darmstadt, Germany), 50 µg/ml 2-phosphate ascorbic acid (Fluka, Ronkonkoma, NY, USA). Media changes were done 3 days a week for 4 weeks. Chondrogenic differentiation was confirmed using Alcian blue staining at acidic pH to show production of sulfate proteoglycans (Mizuno et al., 2002).

2.11. Osteogenesis

hADSCs were seeded at a density of 2×10^4 cells/cm² in DMEM+10% FBS. Twenty-four hours later, the medium was changed to the following osteogenic differentiation medium (adapted from Zuk et al., 2001): DMEM, 10% FBS, 0.1 µM dexamethasone (Merck) and 50 µg/ml ascorbic acid-2-phosphate (Fluka). The medium was refreshed 3 times a week for 4 weeks. The cells were then fixed with 4% PFA, and the alkaline phosphatase activity was detected by staining with 1% Naphthol AS-MX and 1 mg/ml Fast Red-TR.

2.12. Myogenesis

The cells were seeded at a density of 10^3 cells/cm² in DMEM+10% FBS. Twenty-four hours later, the medium was changed to the following myogenic differentiation medium (adapted from Zuk et al., 2001): DMEM, 10% FBS, 50 µM hydrocortisone (Sigma), 10% FBS and 5% horse serum (HS, Sigma). The medium was refreshed 3 times a week for 6 weeks. The cells were then fixed with PFA 4% and immunostained for sarcomeric actin (see above).

2.13. Adipogenesis

The cells were seeded at a density of 3×10^3 cells/cm² in DMEM+10%FBS. Twenty-four hours later, the medium was changed to the following adipogenic differentiation medium (Lin et al., 2005): DMEM 10% FBS, 500 µM isobutylmethylxanthine (IBMX, Sigma), 1 µM dexamethasone (Sigma) and 1 µM indomethacin (Sigma). A total of 10 µM of insulin (Actrapid, Novo Nordisk A/S, Bagsværd, DK) was added for 24 h every 3 days. Differentiation was maintained for 15 days, after which the presence of lipidic intracellular vacuoles was revealed by Oil Red O staining and Cole's hematoxylin counterstaining.

2.14. Cardiomyogenesis

2.14.1. Direct coculture with mouse embryo cardiomyocytes

The c-Kit⁺ and c-Kit⁻ hADSC cells were separately seeded at a density of 7500 cells/cm², together with a disaggregated mouse heart (see above). The differentiation medium (DMEM, 10% FBS, 5% HS, 1% Pen/Strep, 0.1% Fungizone) was changed 3 times a week. The human cells were previously labeled with CM-Dil (Invitrogen). After 3 weeks of coculture, the differentiation was evaluated by observing CM-Dil positive cells in aggregates showing autonomous contraction. The cells were then trypsinized and reseeded in an area 4 times larger for 48 h before being fixed in paraformaldehyde. Differentiation was confirmed by GATA-4 detection by immunofluorescence.

2.14.2. Indirect coculture with mouse embryo cardiomyocytes (transwells)

A mixture of disaggregated mouse fetal heart was seeded in a 2-cm² tissue culture well while 15×10^3 c-Kit⁺ or c-Kit⁻ hADSCs were seeded on a transwell (Corning, Corning, NY, USA) located in the same well, thus providing conditioned medium. Cells were cultivated in DMEM, 10% FBS, 5% HS, 1% P/S for 6 days, with the medium refreshed every 2 days. Cells grown on the well surface were then fixed in 4% PFA and stained for GATA4. The experiment was also repeated by seeding the cells the other way around.

2.14.3. 5-AZA-induced differentiation

The c-Kit⁺ or c-Kit⁻ hADSCs were seeded at a density of 7.5×10^2 cells/cm² in DMEM, 10% FBS and 1% P/S. Twenty-four hours later, 3 µM 5-Azacytidine (5-Aza, Sigma) was added for 48 h. The medium was then changed to DMEM, 10% FBS, 5% HS, 1% P/S and 3-µM 5-Aza for 14 days, with the medium refreshed every 2 days. Cells were then fixed with 4% PFA and stained for GATA4.

2.15. Pancreatogenesis

hADSCs subpopulations were seeded at a density of 8×10^3 cells/cm² in Scholz et al. (2009): DMEM high glucose (Gibco), 1% P/S, 2% B-27 (Gibco), 1 nM Activin A (Sigma), 10 nM Nicotinamide (Sigma), 1 mM β-Mercaptoethanol (Sigma), 2 nM Betacellulin (Sigma), and 10 nM exendin-4. Medium was refreshed every 2 days and after 7 days cells were fixed in 4% PFA and immunostained for insulin.

2.16. Hepatogenesis

2×10^4 of each subpopulation of hADSC cells/cm² were seeded in 60% DMEM Low Glucose (Gibco), 40% MCDB-201 (Sigma), 1% ITS (Gibco), 10^{-9} M dexamethasone (Sigma), 10^{-4} M ascorbic acid-2-phosphate (Sigma), 10 ng/ml rhEGF (R&D Systems), 5% FBS (Gibco), 1% Pen/Strep (Gibco) and 0.6% GlutaMAX (Gibco) in wells covered by a layer of 0.1% gelatin. After 48 h, the medium was changed to a

differentiation medium (the same medium but without EGF and with 10 ng/ml hepatocyte growth factor (HGF, Sigma) and 10 ng/ml oncostatin M (Sigma)). The medium was refreshed every 2 days. After 10 days, the cells were fixed in 4% PFA and immunostained for albumin.

2.17. Telomerase activity

Telomerase activity was quantified using a TRAPEze telomerase detection kit (Millipore Corporation, Billerica, USA), according to the manufacturer's protocol. Briefly, 15×10^4 cells were lysed in 200 μ l of ice-cold Chaps lysis buffer. After 30 min of incubation on ice, the lysates were centrifuged at 12,000g for 20 min at 4 °C, and the supernatant was recovered. The telomeric repeat amplification protocol (TRAP) reaction was performed using the supernatant corresponding to 10,000 cells. Telomere extension was performed at 30 °C for 30 min, followed by 38 cycles of a three-step PCR (94 °C for 30 s, 59 °C for 30 s, and 72 °C for 1 min). The final extension step was performed at 72 °C for 3 min. A standard curve of telomerase activity was generated with TSR8 control templates provided by the kit at different concentrations. In all the PCRs, a 36-base pair template was included as the internal control. In addition, telomerase positive cells provided by the kit were tested as positive controls, and Chaps buffer was tested as negative control for the presence of primer-dimer PCR artifacts and PCR contamination carried over from other samples. TERT activity was measured by examination of 96-well plates in a fluorescence plate reader (Synergy 4, BioTek Instruments, Winooski, USA).

2.18. RT-PCR and Q-PCR

The c-Kit⁺ or c-Kit⁻ hADSC RNA, as well as positive control cell line Jurkat cells (immortalized line of human T lymphocyte cells at passage 14) was extracted with TRIzol (Sigma). Two micrograms of the RNA were retrotranscribed with the Super-Script™ First-Strand Synthesis System for RT-PCR (Invitrogen) according to the manufacturers' protocol. Five microliters of cDNA were amplified with the HotStarTaq DNA polymerase kit (Qiagen) in a PCR using the following cycles: 95 °C 15', (94 °C 45", 56 °C 30", 72 °C 45") \times 40 and 72 °C 7'. To amplify the hTERT cDNA, the primers LT5 (5'-CGGAAGAGTGTCTGGAGCAA-3') and LT6 (5'-GGATGAAGCGGAGTCTGGA-3') were used (Meeran et al., 2010). The expected product was analyzed by agarose gel electrophoresis.

In order to analyze the hTERT levels by q-PCR, we used the primers ht3_FWD (5'-AAATGCGCCCTGTTCT-3') and ht3_REV (5'-CAGTGGCTTGGAGGCA-3') (Shen et al., 2009). To normalize the levels of expression in the various cell types, we used β -actin amplified with the primers hACT_FWD (5'-AACCGGAGAAGATCACCCAGATCATGTTT-3') and hACT_REV (5'-AGCAGCCGCATCTCTTGCTCGAAGTC-3'). Reactions were assembled with the Quantimix Easy kit (BioTools) and run in a LightCycler system (Roche).

The crossing points of the amplification curves were determined with the LightCycler Quantification Software (Roche) using the second derivative method. To quantify the levels of expression, we used the formula $EXP(-\Delta Cp \text{ hTERT-Act})$.

2.19. Images and videos

Pictures were either taken with a Nikon camera (Nikon Corporation, Tokyo, Japan) mounted on a Zeiss inverted microscope and processed with the software Nis-elements (Nikon) or taken with an Olympus camera (Olympus Corporation, Tokyo, Japan) mounted on an Olympus microscope and analyzed with the DP software (Olympus).

Videos were taken using a Hamamatsu (Hamamatsu Photonics K.K., Tokyo, Japan) camera with a Leica inverted microscope and processed with the LAS AF software (Leica Microsystems).

2.20. Quantification, image analysis and statistical analysis

Upon immunostaining, at least 500 random cells were counted per well and condition. In the case of myogenic and osteogenic induction, 200 \times pictures of 10 different fields per condition were taken, and the optical density was analyzed with the Motic Images Advanced version 3.2 software (Motic China Group Co., China). Significance ($p < 0.05$) was evaluated with the Mann-Whitney *U* test using the IBM SPSS Statistics 2.0 software.

3. Results

3.1. The human adipose tissue SVF contains a subpopulation of c-Kit positive cells that only partially overlaps with CD105 ADSCs

Using double immunolabeling and FACS analysis, three populations were isolated, either c-Kit or CD105 in isolation or double positive for both markers (Fig. 1A). The total c-Kit positive population varied between samples, and accounted for a mean of 0.5% of the SVF (Fig. 1A and B), in contrast to the 9–14% of the CD105⁺ population, indicating that the c-Kit population is very scarce and that most SVF cells (99.5%) are c-Kit negative. The percentage of c-Kit positive cells was maintained during the first passages in whole cultured SVF (Fig. 1B).

3.2. C-Kit ADSCs have clonogenic capacity

C-Kit positive cells were isolated by FACS, and one cell per well was cultured on Terasaki plates, giving rise to clones (Fig. 4A) that lasted for at least 8 months in culture until reaching quiescence. At that time, most cells had lost c-Kit expression, although a small percentage still remained c-Kit positive (not shown).

3.3. C-Kit ADSCs have higher proliferative ability and self-renewal capacity

The proliferation index by BrdU incorporation was measured at 100, 200 and 300 days of culture in c-Kit positive versus c-Kit negative populations isolated by FACS, revealing a higher proliferation index for the c-Kit positive population at all measuring times (Fig. 2). In agreement with this, the c-Kit positive population showed a statistically longer proliferation period (not shown).

3.4. C-Kit ADSCs show higher telomerase activity and telomerase expression

The higher proliferative ability and higher self-renewal capacity of the c-Kit positive cells suggested that the c-Kit positive population may have higher telomerase activity. To confirm this directly, we measured the telomerase activity in both c-Kit positive and negative subpopulations, confirming that the c-Kit⁺ displayed higher telomerase activity (Fig. 3A). Furthermore, we measured the telomerase expression by quantitative PCR, which confirmed that only the c-Kit positive population showed detectable telomerase (Fig. 3B).

3.5. C-Kit ADSCs are located in the perivascular niche

Immunohistochemistry anti-c-Kit was performed in sections of human adipose tissue, revealing the c-Kit positive cells as large cells with large cytoplasm and always located near blood vessels (Fig. 4B).

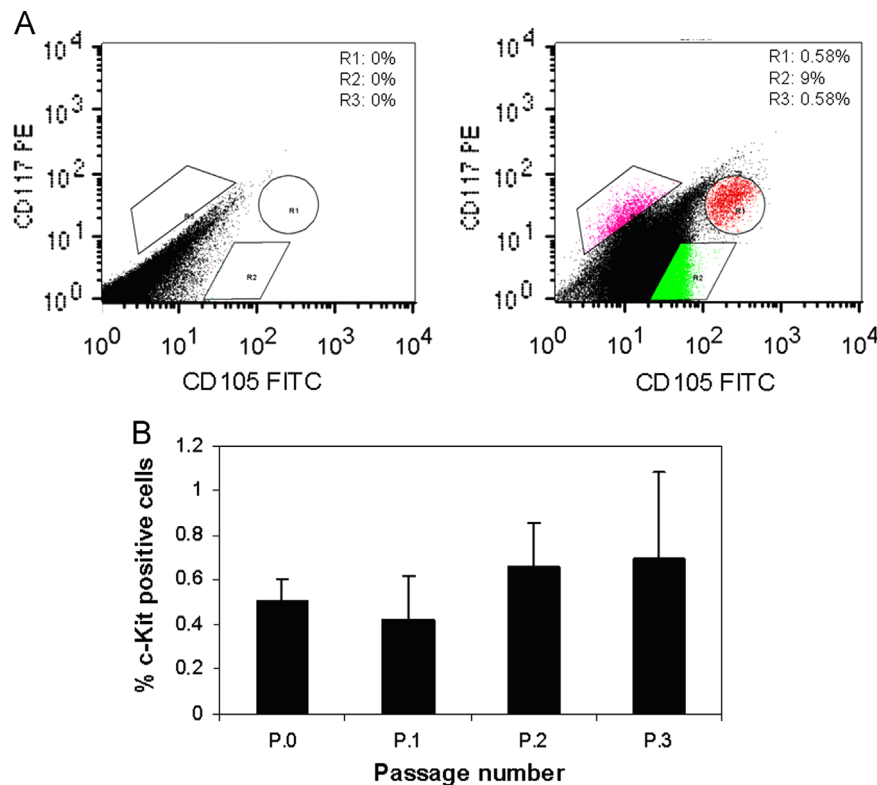


Fig. 1. Fluorescence-activated cell sorting of a sample of the stromal vascular fraction of human adipose tissue. (A) Isotype negative control (left panel) and CD105/C-Kit (right panel) sorted cells. R1: CD105+/c-Kit+. R2: CD105+/C-Kit-. R3: CD105-/C-Kit+. Percentages of each population are given within the graph. (B) The percentage of c-Kit (CD117) positive cells maintained during passaging. Data shows mean and standard deviation of three different samples.

3.6. C-Kit ADSCs are resident in the adipose tissue

To rule out the possibility that the c-Kit population was not resident in the adipose tissue but instead a blood population (e.g. fibrocytes), SVF was isolated from mice that had undergone perfusion with PBS and therefore had all of their blood extracted prior to adipose tissue extraction. The SVF was then analyzed by FACS. The results show that the c-Kit population remained in the blooded-out adipose tissue, demonstrating that c-Kit cells are resident in the adipose tissue (Fig. 4C to E).

3.7. C-Kit ADSCs show similar osteogenic and myogenic mesodermal potential

We then performed directed differentiation analysis to demonstrate the differentiation potential of the c-Kit positive population for chondrogenesis, osteogenesis and myogenesis. The c-Kit subpopulations did in fact differentiate towards these three lineages (Fig. 5A, B and D), although at the same levels as the c-Kit negative cells (Fig. 5C and E), independently of CD105 expression. In the case of chondrogenic differentiation, efficiency could not be measured due to the micromass technique used to direct differentiation.

3.8. C-Kit ADSCs show higher adipogenic potential, but they are not CD24 preadipocytes

The c-Kit positive cells also showed adipogenic potential when cultured in the appropriate medium (Fig. 6A), revealing statistically higher adipogenic potential than the c-Kit negative cells, and independently of CD105 expression (Fig. 6B). To determine whether the c-Kit population was the same as the preadipocytes (although improbable due to the higher self-renewal and telomerase levels shown above), we performed double immunohistochemistry for c-Kit and the

preadipocyte marker CD24 (Rodeheffer et al., 2008; Berry et al., 2013) and demonstrated that they are in fact different subpopulations of the SVF (Fig. 6C and D).

3.9. C-Kit ADSCs show similar cardiomyogenic differentiation potential, but they exert higher maintenance of cardiac characteristics in mouse embryonic cardiomyocytes

In order to show the pluripotency of the c-Kit positive cells, the differentiation potential outside the mesodermal lineages was measured by directed differentiation towards cardiomyogenesis. Several methods were performed: The first method employed directed chemical differentiation with 5-azacytidine, achieving an efficiency of differentiation of a mean of about 20% GATA4 positive cells in the c-Kit+ population, a percentage slightly but not significantly higher than that achieved by the c-Kit negative population (Fig. 7A and B). The second method employed a coculture of c-Kit positive or negative cells with mouse embryonic cardiomyocytes, which resulted in spontaneously contractile mixed colonies during the whole period of coculture in all cases (Video 1). Cardiomyogenic differentiation of the c-Kit+ ADSCs was in fact achieved (Fig. 7C) in approximately 30% of the cells, but again no statistical difference was revealed with respect to the c-Kit negative cells (Fig. 7D). In contrast, the c-Kit positive cells exerted a positive action on the embryonic cardiomyocytes, which helped to maintain the marker GATA4 in the mouse embryonic cardiomyocytes and, in fact, preserved a higher percentage of positive cells when sharing supernatant cultured in transwells with c-Kit positive cells (Fig. 7E and F).

Supplementary material related to this article can be found online at <http://dx.doi.org/10.1016/j.diff.2014.02.007>.

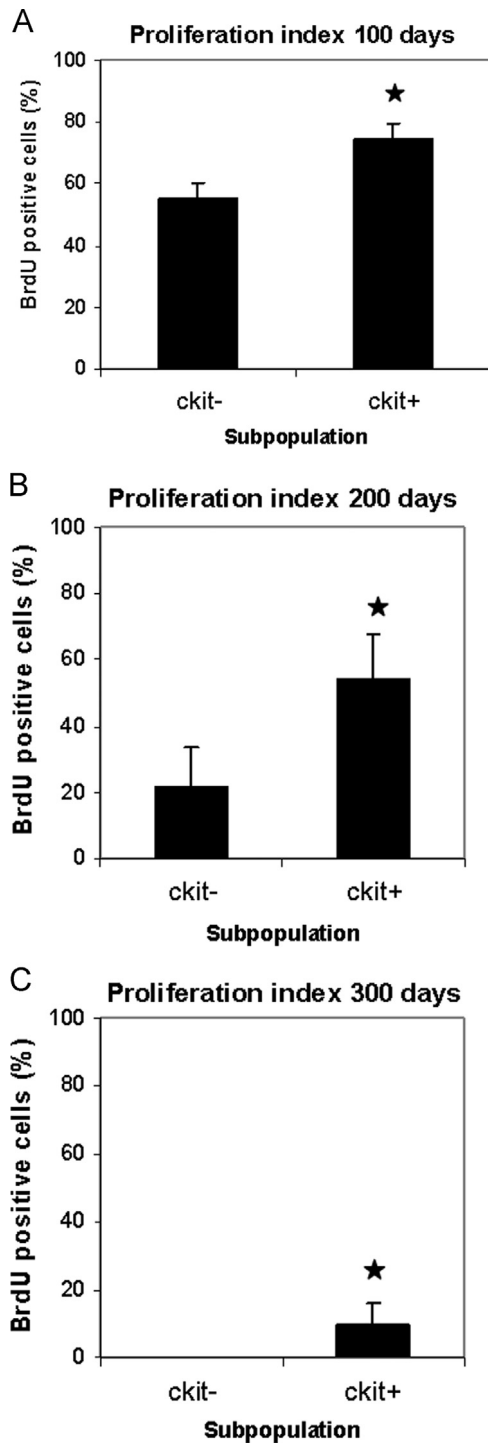


Fig. 2. Proliferation index by BrdU incorporation of the human stromal vascular fraction c-Kit positive and negative populations at various culture time points. (A) 100 days. (B) 200 days. (C) 300 days. Data shows mean and standard deviation of one representative experiment performed in triplicate. Stars indicate significant difference at $p < 0.05$.

3.10. C-Kit ADSCs show higher pancreatic endodermal potential

The pancreatogenic potential, measured by the presence of insulin producing cells, was also higher for the c-Kit positive subpopulations independently of CD105 expression (Fig. 8A and B), demonstrating that the c-Kit+ population has a higher differentiation potential not only to some mesodermal lineages but also to endodermal lineages.

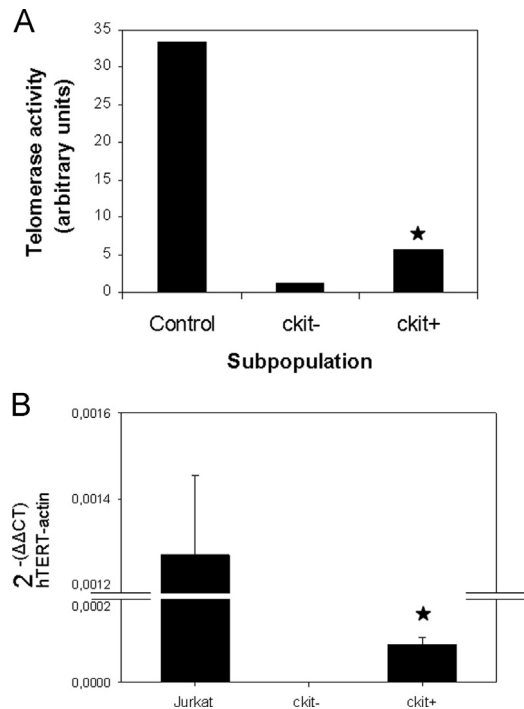


Fig. 3. (A) Fluorometry of the TERT activity of the human stromal vascular fraction c-Kit positive and negative populations using the TrapezeXL kit. Star indicates significant difference at $p < 0.05$ between c-Kit positive and c-Kit negative subpopulations. (B) Quantitative PCR of the human stromal vascular fraction c-Kit positive and negative populations telomerase expression. Jurkat immortal cell line at passage 14 were used as positive controls. The graph shows the difference in terms of gene expression working out the Delta Delta CT algorithm between TERT and the housekeeping gene actin. Star indicates significant difference at $p < 0.05$ between c-Kit positive and c-Kit negative subpopulations.

3.11. C-Kit ADSCs show higher hepatocyte endodermal potential

To determine further the preferential endodermal differentiation potential, we performed directed differentiation towards the hepatogenic lineage, which resulted in a statistically significant higher percentage (up to 70%) of the c-Kit subpopulations being albumin positive, independently of CD105 expression (Fig. 8C and D).

4. Discussion

We demonstrated higher proliferative activity and self-renewal capacity, which concurs with the higher telomerase expression and higher telomerase activity of the c-Kit positive subpopulation of ADSCs. Until now, no marker had identified the telomerase-expressing cells in the SVF, as we could not detect any telomerase mRNA expression in the c-Kit negative subpopulation. Madonna et al. (2008) identified a subpopulation of MSCs in mouse SVF that coexpressed myocardin A (a key regulator of cardiovascular myogenic development) and telomerase expression and activity, but only 8% of the telomerase positive cells were myocardin A positive as well. We have found a weak telomerase activity in c-Kit negative cells, which we believe is residual, as no telomerase mRNA could be amplified in the RT-PCR. Sachs et al. (2012), could not find either telomerase mRNA or activity in human SVF, probably due to the use of whole SVF and the lower number of cells used for detection. In agreement with our data, cancer cells show even higher telomerase activity than (c-Kit+) ADSCs (Jeon et al., 2011).

Previous studies have found subpopulations of c-Kit cells in freshly isolated SVF: Prunet-Marcassus et al. (2006) and Han et al.

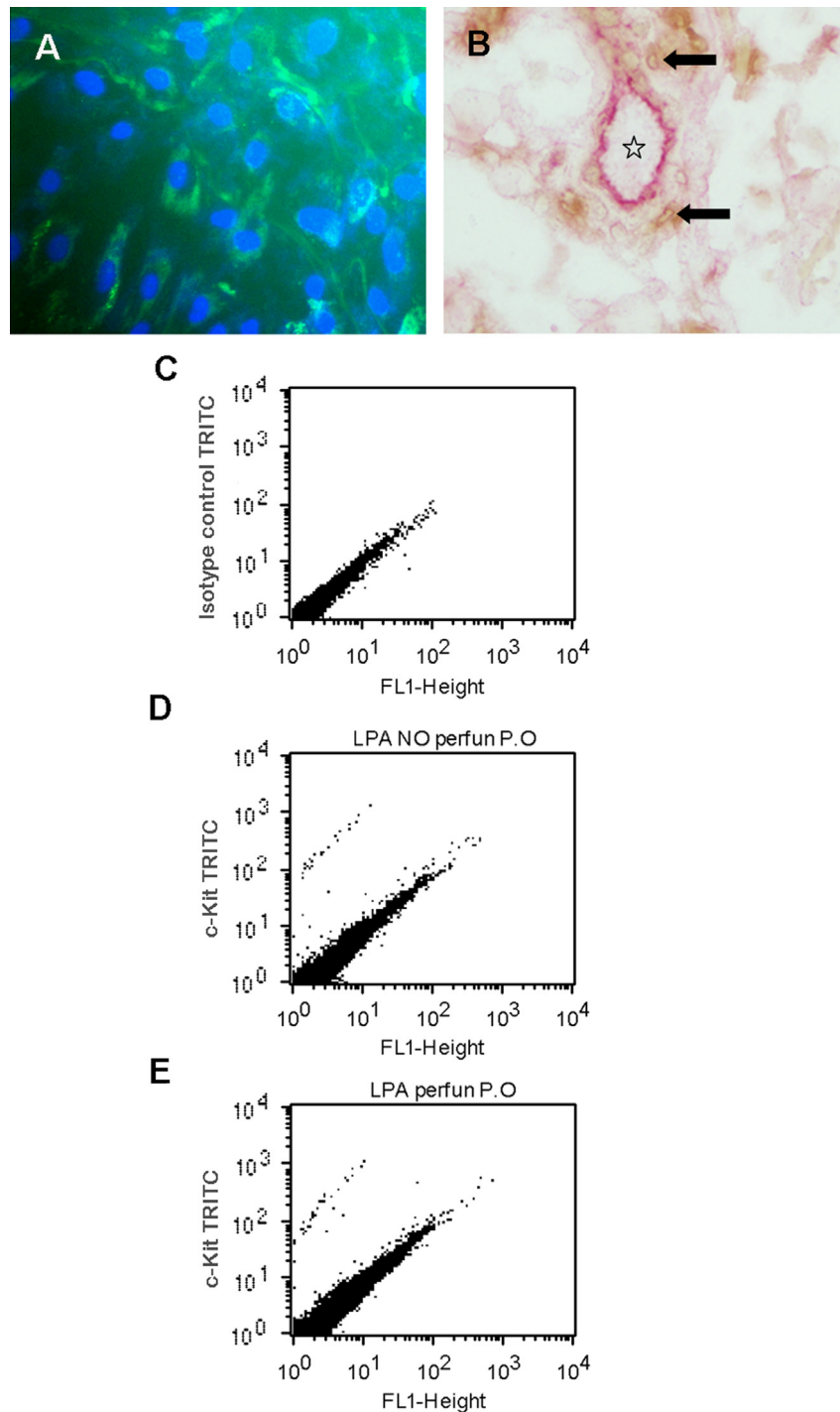


Fig. 4. (A) Immunofluorescence against c-Kit (FITC, green) in a clone derived from one against c-Kit⁺ cell. DAPI shows nuclear stain in blue. 200 \times . (B) Location of the human stromal vascular fraction c-Kit⁺ population. Immunohistochemistry against c-Kit in a human adipose tissue section showing positive cells in the perivascular stroma in brown (arrows) surrounding a blood vessel labeled with anti-CD31 in red (star). Hematoxylin counterstain. 400 \times . (C) Isotype negative control of FACS analysis in mouse stromal vascular fraction. (D) FACS analysis of c-Kit subpopulation in mouse stromal vascular fraction after PBS perfusion showing that the c-Kit population remained in the adipose tissue after perfusion. (For interpretation of the references to color in this figure legend, the reader is referred to the web version of this article.)

(2010) in mouse SVF, and Bai et al. (2007), Varma et al. (2007), De Francesco et al. (2009) and Quirici et al. (2010) in human SVF at similar percentages, but these authors did not further characterize this subpopulation. Recently, Li et al. (2012), isolated c-Kit⁺ cells from hADSC and characterize their cytokine expression but not their differentiation potential. Also, very recently, a c-Kit⁺ spontaneously immortalized cell clone was isolated from mouse SVF and demonstrated to be able to differentiate into

chondrogenic, osteogenic, adipogenic, and cardiogenic phenotypes (Zamperone et al., 2013), but no comparison was made with whole SVF. In bone marrow Mangi et al. (2003), and in heart tissue, Beltrami et al. (2003) and Ellison et al. (2013) found subpopulations of multipotent c-Kit⁺ capable of giving rise to cardiomyocytes. In mouse lung vessels, a isolated population of c-Kit⁺ cells was capable of generating mature blood vessels in vitro (Fang et al., 2012).

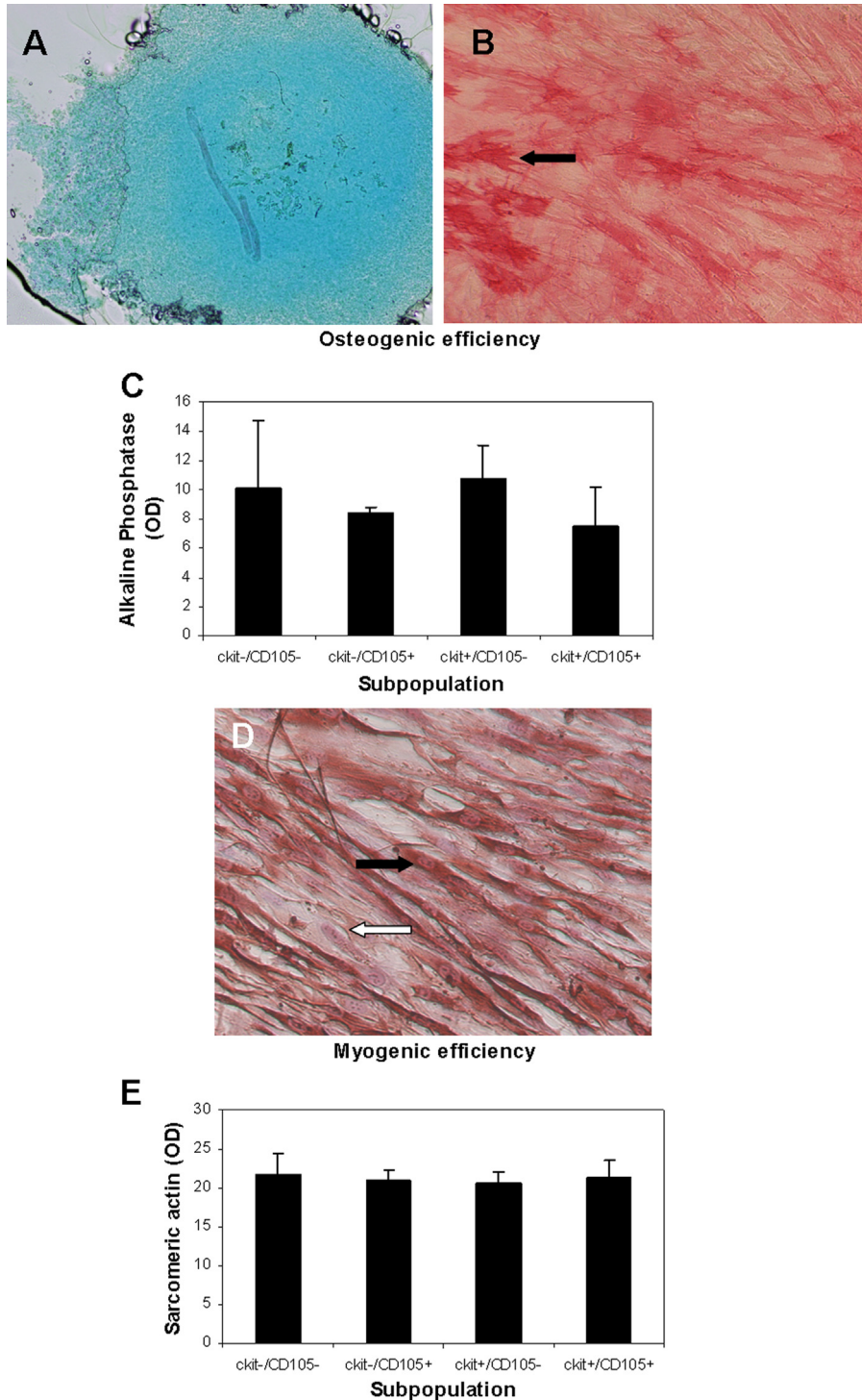


Fig. 5. (A) In vitro chondrogenesis of the human c-Kit positive population, cultured using the micromass technique and revealed by Alcian blue. 100 ×. (B) in vitro osteogenesis of the human stromal vascular fraction c-Kit positive population, revealed by Alkaline phosphatase staining with Fast Red (arrow shows a positive cell). 200 ×. (C) Measurement of differentiation efficiency of the four subpopulations based on c-Kit and CD105 expression. Data shows mean and standard deviation of one representative experiment performed in triplicate. No differences were found. (D) In vitro myogenesis of the human stromal vascular fraction c-Kit positive populations, shown by sarcomeric α -actin immunostaining revealed in brown with DAB, and hematoxylin counterstain in blue. Black arrow shows a positive cell and white arrow shows a negative cell. 200 ×. (E) Measurement of differentiation efficiency of the four subpopulations based on c-Kit and CD105 expression. Data shows mean and standard deviation of one representative experiment performed in triplicate. No differences were found. (For interpretation of the references to color in this figure legend, the reader is referred to the web version of this article.)

To our knowledge, no studies have shown the presence of c-Kit as compared with the classical CD105 in SVF. Our results are in contrast with the results for rat muscle obtained by Young's group who identified multipotent mesenchymal stem cells as CD90 and telomerase positive, with unlimited proliferation potential, and

the tripotent (osteo-chondro-adipoblast) mesenchymal progenitor cells as CD105, c-Kit and CD166 positive and capable of only 8–10 population doublings (50–70 for humans) (Young and Black, 2004; Young et al., 2004). In contrast in our case, the c-Kit+ subpopulation is also telomerase positive, capable of more than 150 population

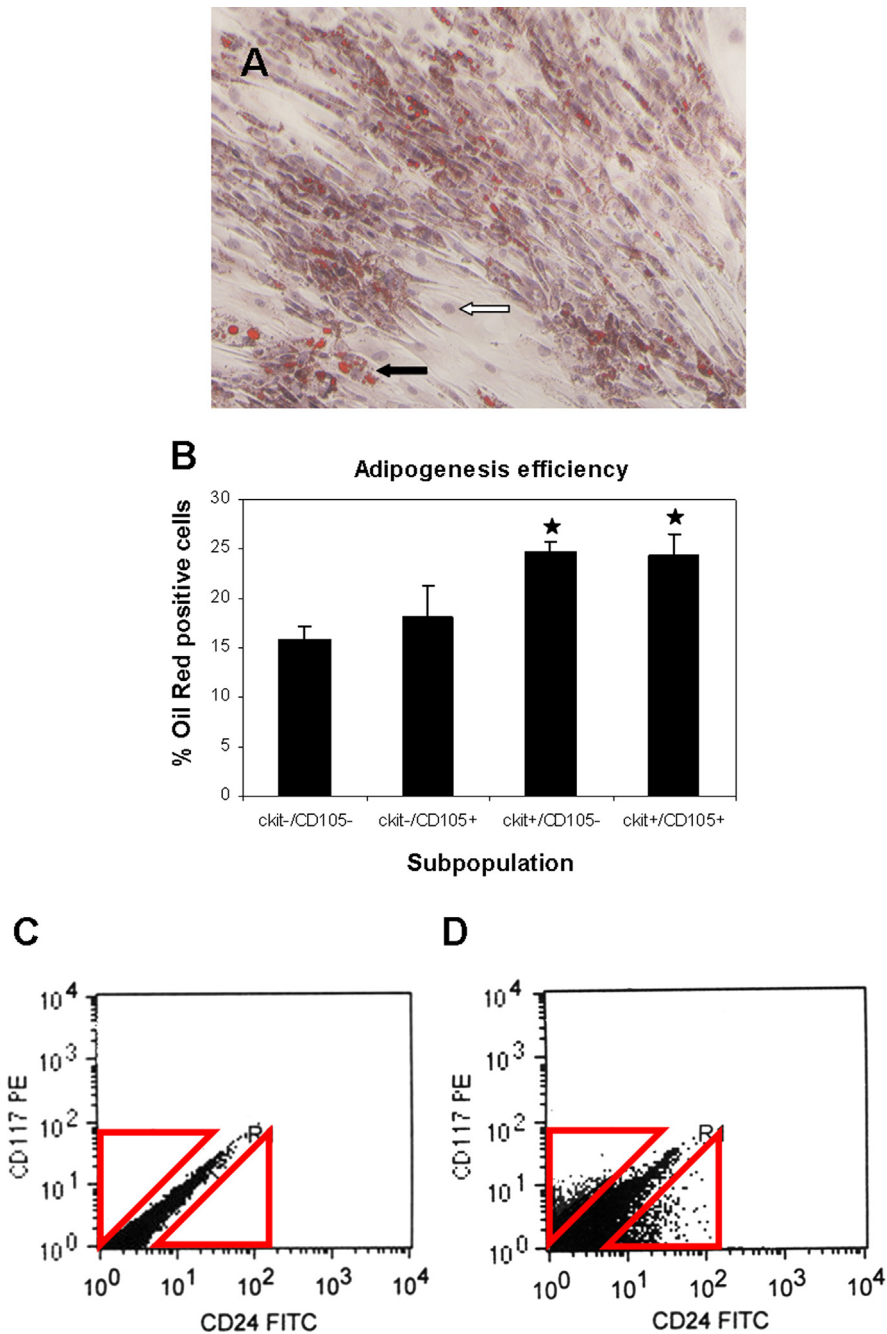


Fig. 6. (A) In vitro adipogenesis of the human stromal vascular fraction c-Kit positive population, revealed by Oil red staining in red. Black arrow shows a positive cell and white arrow shows a negative cell. 200 ×. (B) Measurement of differentiation efficiency of the four populations based on c-Kit and CD105 expression. Data shows mean and standard deviation of one representative experiment performed in triplicate. Star indicates significant difference at $p < 0.05$. (C) Isotype negative control of FACS analysis of the human SVF CD24 (preadipocyte marker) and c-Kit (CD117). (D) Both subpopulations separated by FACS (red triangles) showing that they are distinct subpopulations. (For interpretation of the references to color in this figure legend, the reader is referred to the web version of this article.)

doublings and able to differentiate into cardiomyocytes, hepatocytes and insulin-producing pancreaticocytes, in addition to the osteochondro-adipocytes. Differences could be due to tissue-specific differences or, less likely, to differences between the species. In any case, further studies would be necessary to characterize multipotent mesenchymal versus progenitor cells in human SVF.

4.1. C-Kit ADSCs are located in the perivascular niche

In agreement with our data, Zannettino et al. (2007), Traktuev et al. (2008) and Ryu et al. (2013) found that multipotent ADSCs

show a location similar to that of pericytes. Other authors recently made the same findings in multiple organs (Da Silva Meirelles et al., 2006; Crisan et al., 2008; Lin et al., 2010; Gerlach et al., 2012). The fact that the c-Kit positive population remains in the SVF fraction after PBS reperfusion clearly demonstrates that the c-Kit+ ADSC population is distinct from the circulating fibrocytes with adipogenic potential (Hong et al., 2005).

In vitro adipogenic differentiation efficiency varies among studies (Yoshimura et al., 2006; Zuk et al., 2001; Cao et al., 2005; Sakaguchi et al., 2005; Wosnitza et al., 2007). A high heterogeneity among donors has been reported, with 30% to 80%

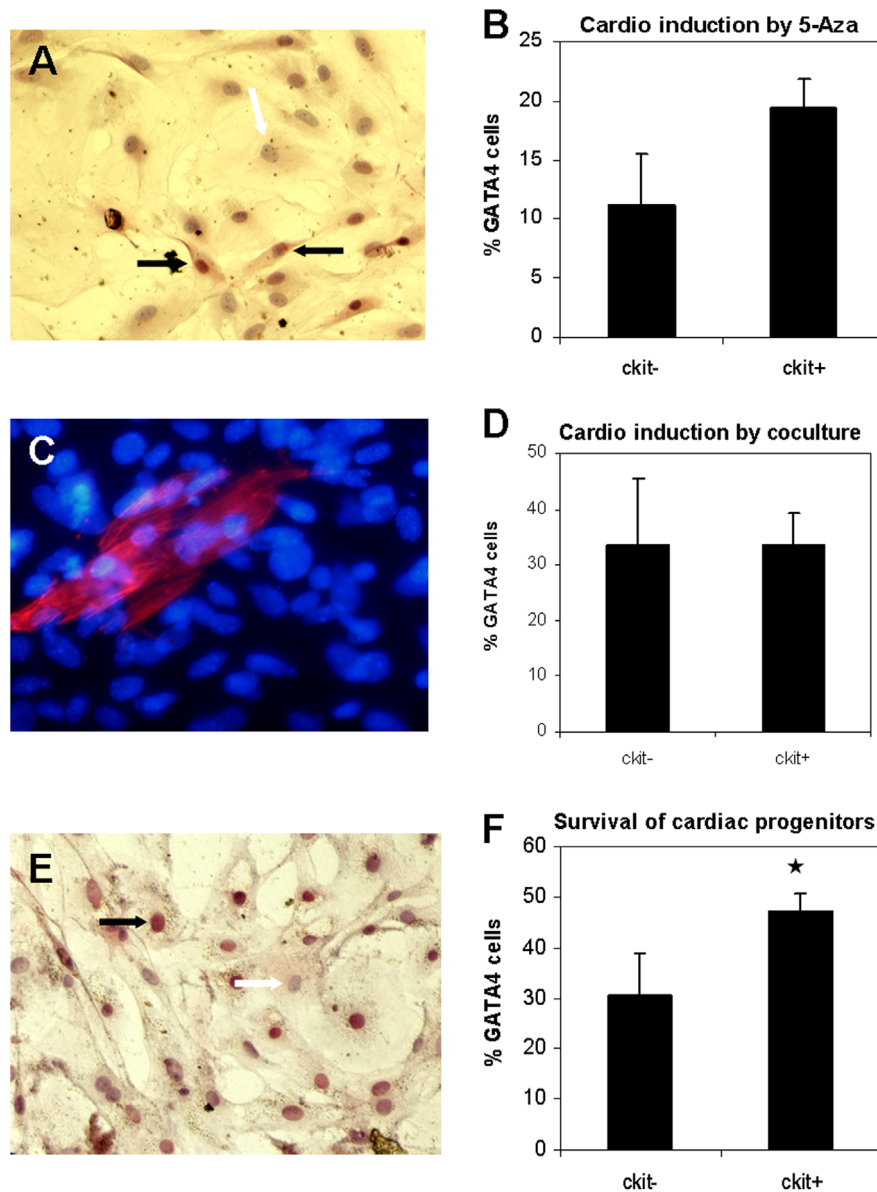


Fig. 7. (A) In vitro cardiomyogenesis by 5-azacytidine of the human stromal vascular fraction c-Kit positive population, revealed by GATA4 nuclear immunostaining in brown with DAB and hematoxylin counterstain. Black arrows: DAB (brown) positive cells. White arrow: Hematoxylin (blue) negative cell. $200\times$. (B) Measurement of differentiation efficiency. Data shows mean and standard deviation of one representative experiment performed in triplicate. No differences were found. (C) In vitro cardiomyogenesis of the human stromal vascular fraction c-Kit positive population by coculture with mouse embryonic cardiomyocytes, revealed by immunofluorescence against human troponin (red fibers, positive cell), and DAPI nuclear counterstain (negative cells). $\times 400$. (D) Measurement of differentiation efficiency. Data shows mean and standard deviation of one representative experiment performed in triplicate. No differences were found. (E) In vitro mouse embryonic cardiomyocyte progenitor maintenance by incubation with the c-Kit positive population conditioned medium in transwells, revealed by GATA4 nuclear immunostaining and hematoxylin counterstain. Black arrow: DAB (brown) positive cell. White arrow: Hematoxylin (blue) negative cell. $200\times$. (F) Measurement of differentiation efficiency. Data shows mean and standard deviation of one representative experiment performed in triplicate. Star indicates significant difference at $p < 0.05$. (For interpretation of the references to color in this figure legend, the reader is referred to the web version of this article.)

Nile Red positive cells after 2 weeks of differentiation (Sen et al., 2001). We found a mean of 25% and a maximum of 65% in the c-Kit⁺ subpopulation, which was statistically significantly higher than the rest of the SVF (c-Kit negative subpopulations).

In vivo, coinjection of ADSCs with adipose tissue has been performed for aesthetic purposes (Ko et al., 2011), demonstrating longer stability for the adipose implant in nude mice. Several clinical trials have been performed with this procedure in humans, mainly for breast augmentation/reconstruction and facial reconstruction with autologous fat enriched with ADSCs (Yoshimura et al., 2010, 2008a, 2008b; Lee et al., 2012; Gentile et al., 2012; Pérez-Cano et al., 2012). In all of these studies, volume restoration was successful and achieved significantly better results than with

fat transplantation alone; however, the volume was partially lost after 1 year. The use of the isolated c-Kit⁺ subpopulation (both CD105 positive and negative) with higher adipogenic differentiation potential might improve these results.

4.2. In vitro cardiomyogenic differentiation efficiency

By coculture with mouse embryonic cardiomyocytes, we found a mean of 37% cardiomyogenic differentiation. Other authors have achieved a somewhat lower efficiency (Gaustad et al., 2004; Metzle et al., 2011) when coculturing with neonatal or adult rat cardiomyocytes. Although we found no differences between the subpopulations, we did find better efficiency when coculturing

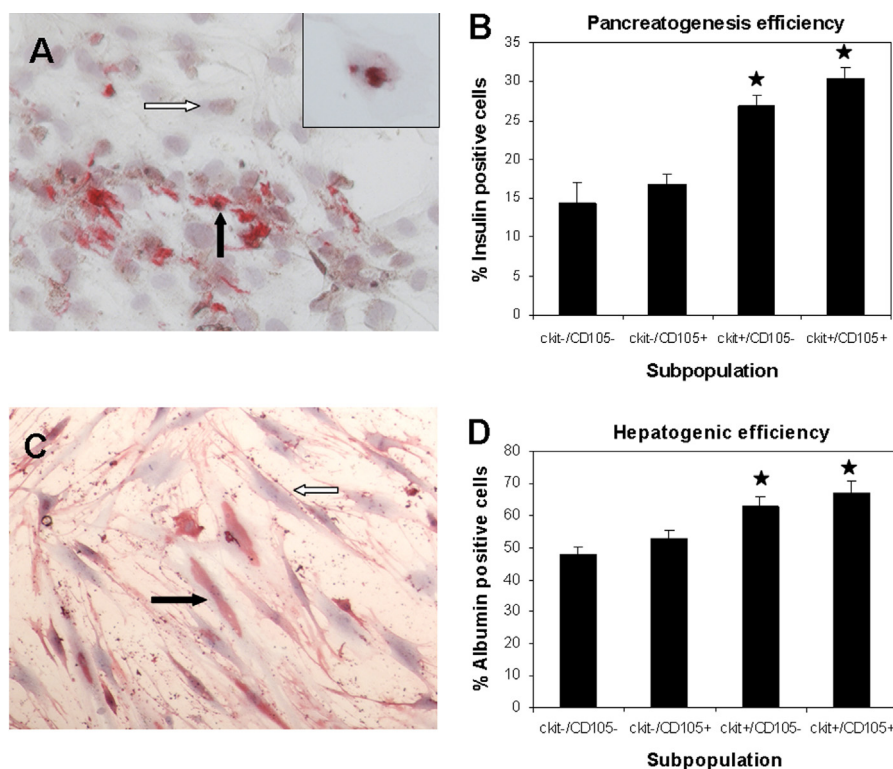


Fig. 8. (A) In vitro pancreatogenesis of the human stromal vascular fraction c-Kit positive population, revealed by insulin immunostaining (Fast Red) and hematoxylin counterstain. Black arrow shows a positive cell and white arrow shows a negative cell. 200 \times . Inset shows higher magnification of one cell with an insulin granule. 400 \times . (B) Measurement of differentiation efficiency of the four subpopulations based on c-Kit and CD105 expression. Data shows mean and standard deviation of one representative experiment performed in triplicate. Stars indicate significant difference at $p < 0.05$. (C) In vitro hepatogenesis of the human stromal vascular fraction c-Kit positive population, revealed by albumin cytoplasm immunostaining (Fast Red) and hematoxylin counterstain. Black arrow shows a positive cell and white arrow shows a negative cell. 200 \times . (D) Measurement of differentiation efficiency of the four populations based on c-Kit and CD105 expression. Data shows mean and standard deviation of one representative experiment performed in triplicate. Stars indicate significant difference at $p < 0.05$. (For interpretation of the references to color in this figure legend, the reader is referred to the web version of this article.)

with embryonic cardiomyocytes instead of the more differentiated neonatal cardiomyocytes. This might improve the outcome of in vivo experiments because cells that feature a true cardiomyogenic phenotype may have the potential for ensuring a true regeneration of dead myocardium (Menasché, 2005). In fact, depletion of myocardial resident c-Kit⁺ cells from mouse heart abolished cardiac regeneration and functional recovery in an experimental model of myocardial infarct (Ellison et al., 2013).

We achieved up to 45% maintenance of the cardiac progenitor phenotype when cultured with c-Kit⁺ ADSCs in transwells; therefore, the supernatant of c-Kit⁺ cells from SVF might serve a cardioprotective role in vivo. In fact, the primary effect of mesenchymal cells is to secrete a wide variety of growth factors, which likely makes them more suitable for paracrine-enhancing angiogenesis than for generating intrinsically contractile cells (Murry et al., 2004; Alvarez-Dolado et al., 2003; Kinnaird et al., 2004; Paul et al., 2012; Kim et al., 2012; Li et al., 2012). Interestingly, the cardiac c-Kit⁺ cell population increases in response to ischemic injury and contributes to in vivo cardioprotection (Altarache-Xifró et al., 2009). In addition, when SVF is preconditioned with cardiomyocyte-conditioned medium (Bai et al., 2007) or specifically with EGF and PDGF (Chang et al., 2011), more c-Kit⁺ cells are found, and these cells improve the myocardial function in infarcted rats (Chang et al., 2011). Our data provides further support for ADSCs as a valuable tool for cell therapy for the ischemic heart, in particular, c-Kit⁺ secreted factors might improve the outcome.

4.3. In vitro differentiation efficiency to pancreatic cells

Our data showed up to 39% insulin-producing cells differentiation efficiency achieved by the c-Kit⁺/CD105⁺ subpopulation after only one week in culture, a statistically significant increased capability respect to the rest of the SVF. Kucia et al. (2006) using a previous protocol and BM-derived VSEL achieved very low efficiency as revealed by c-peptide immunofluorescence. With improved protocols and ADSCs, Timper et al. (2006) and Scholz et al. (2009) – with the same protocol used in this study, – achieved better efficiencies, assessed by dual morphological characterization and competitive chemiluminescent enzyme immunoassay for insulin peptide at 2 weeks in culture. Differences with our data could be due to differences in the protein chosen to reveal the pancreatic phenotype, the method of detection as well as the duration of the differentiation period.

In vivo, injection of transfected mADSCs with Pdx-1 pancreatic differentiation transcription factor into the pancreas of streptozotocin-injured mice promoted the differentiation of the mADSCs into insulin and c-peptide secreting cells and partially restored the pancreatic function (Lin et al., 2009; Kajiyama et al., 2010). Moreover, when clonal populations of human or mouse ADSCs are predifferentiated into insulin-producing cells in vitro, and injected peritoneally in mice, the glycemic index was nearly restored (Chandra et al., 2009, 2011). The use of the c-Kit⁺ subpopulations, previously differentiated into insulin-producing cells, could further improve these results.

4.4. *In vitro* differentiation to hepatocytes efficiency

We achieved up to 70% efficiency in the hepatocyte differentiation of the c-Kit⁺/CD105⁺ subpopulation, measured by albumin production after only 10 days, a remarkable improvement compared with previous studies using CD105⁺ cells (presumable c-Kit negative) (Banas et al., 2009).

Banas et al. (2007) have shown that both naïve and predifferentiated human ADSCs integrate *in vivo* in the hepatic parenchyma 24 h after injection of the ADSCs in mice with CCl₄ chemical hepatic damage. Longer-term studies (Aurich et al., 2009) have shown a remarkably increased engraftment (10 ×) of the predifferentiated hADSCs when compared with undifferentiated hADSCs. In terms of hepatic regeneration, mice with CCl₄ chemical hepatic damage achieved significantly lower levels of ammonia, aspartate aminotransferase, alanine aminotransferase and uric acid 24 h after injection of the ADSCs. This was accomplished with only 20% efficiency of *in vitro* differentiation (Banas et al., 2009). The use of the c-Kit⁺ subpopulations, with a mean of 70% *in vitro* differentiation efficiency, could improve this type of treatment. In a recent study (Wang et al., 2012), undifferentiated rat ADSCs lowered fibrosis and improved microcirculation in rats with hepatic damage after 6 weeks, but no data was provided regarding engraftment. Again, we expect the use of the c-Kit⁺ subpopulation to further improve these results.

We believe that the higher differentiation efficiency towards endodermal lineages of the c-Kit⁺ cells is due to the lower differentiated state of this subpopulation than the rest of the SVF. In other tissue settings, Fang et al. (2012), describe a c-Kit⁺CD105⁺(Lin-CD31⁺) population isolated from lung vasculature corresponding to a subpopulation of endothelial progenitors which are clonogenic, and capable of generating functional blood vessels. Bearzi et al. (2009), found isolated c-Kit⁺ cells in human heart vascular walls, which show stem cell characteristics such as clonogenicity and self-renewal, and higher endothelial, smooth muscle and cardiomyogenic potential. Our data also shows that the c-Kit⁺ population is isolated in the SVF from perivascular locations and show higher differentiation potential as well. In accordance to our hypothesis, Gupta et al. (2012) and Tran et al. (2012), by *in vivo* cell tracing, demonstrate that in adult adipose tissue, endothelial cells give rise to pericytes which in turn give rise to MSC. Then MSC differentiate into preadipocytes and adipocytes when necessary. All these data suggests that cells closer to endothelial progenitors are less differentiated and support higher differentiation potential.

The differentiation potential of other ADSC subpopulations has been previously characterized in a number of studies. Sengenès et al. (2007) isolated a subpopulation (CD34⁺/CD31⁻) that could differentiate into the endothelial lineage. Rada et al. (2011) demonstrated the higher osteogenic potential exhibited by cells isolated by Stro1 and the higher chondrogenic potential by CD105 and CD29. Traktuev et al. (2008) found that CD34⁺/CD31⁻/CD140⁺ ADSCs enhanced the stabilization of endothelial networks when cocultured with endothelial cells. Quirici et al. (2010) isolated a L-NGFR⁺ subpopulation that showed an increased cell proliferation rate as well as increased adipogenic, chondrogenic and osteogenic potential. Interestingly, a high percentage (66%) of L-NGFR also coexpressed c-Kit, but these authors did not study the L-NGFR⁺ subpopulation's endodermal differentiation potential.

In conclusion, our data suggests that the isolation of ADSC subpopulations with anti-c-Kit antibodies allows for the selection of a more homogeneous subpopulation with higher telomerase activity and expression, increased adipogenic potential, increased cardioprotective properties and a higher proliferative and endodermal differentiation potential, providing a

useful tool for specific therapies in regenerative medicine applications.

Conflict of interest

The authors declare no potential conflicts of interest.

Acknowledgements

This work was supported in part by grants PI-308 and CP-03/00007 from the Fondo de Investigaciones Sanitarias (Healthcare Research Fund), Ministry of Health, Spain, SAF2010-19230 from the Ministry of Economy and Competitiveness, Spain, from the BioMedical Foundations Mutua Madrileña and Marató TV3, Spain. The authors wish to acknowledge Fernando Nuñez (IIB) for his assistance with the mouse perfusion, Fátima Domínguez (LIC) for the SVF processing, Mar Royuela (UA) for image analysis, IdiPAZ BioBank for sample custody, Mariana Diaz-Almirón (Biostatistics Section, Hospital La Paz) for statistical analysis, and Juliette Siegfried (ServingMed.com) for the English editing of this manuscript.

Appendix A. Supporting information

Supplementary data associated with this article can be found in the online version at <http://dx.doi.org/10.1016/j.diff.2014.02.007>.

References

- Altarache-Xifró, W., et al., 2009. Cardiac c-kit+AT2+ cell population is increased in response to ischemic injury and supports cardiomyocyte performance. *Stem Cells* 27 (10), 2488–2497.
- Alvarez-Dolado, M., et al., 2003. Fusion of bone-marrow-derived cells with Purkinje neurons, cardiomyocytes and hepatocytes. *Nature* 425 (6961), 968–973.
- Arnalich-Montiel, F., et al., 2008. Adipose-derived stem cells are a source for cell therapy of the corneal stroma. *Stem Cells* 26 (2), 570–579.
- Aurich, H., et al., 2009. Hepatocyte differentiation of mesenchymal stem cells from human adipose tissue *in vitro* promotes hepatic integration *in vivo*. *Gut* 58 (4), 570–581.
- Bai, X., et al., 2007. Genetically selected stem cells from human adipose tissue express cardiac markers. *Biochem. Biophys. Res. Commun.* 353 (3), 665–671.
- Banas, A., et al., 2009. Rapid hepatic fate specification of adipose-derived stem cells and their therapeutic potential for liver failure. *J. Gastroenterol. Hepatol* 24 (1), 70–77.
- Banas, A., et al., 2007. Adipose tissue-derived mesenchymal stem cells as a source of human hepatocytes. *Hepatology* 46 (1), 219–228.
- Bearzi, C., et al., 2009. Identification of coronary vascular progenitor cell in the human heart. *Proc. Nat. Acad. Sci. U.S.A* 106, 15885–15890.
- Beltrami, A.P., et al., 2003. Adult cardiac stem cells are multipotent and support myocardial regeneration. *Cell* 114 (6), 763–776.
- Berry, D.C., et al., 2013. The developmental origins of adipose tissue. *Development* 140 (19), 3939–3949.
- Boquest, A.C., et al., 2005. Isolation and transcription profiling of purified uncultured human stromal stem cells: alteration of gene expression after *in vitro* cell culture. *Mol. Biol. Cell* 16 (3), 1131–1141.
- Cao, Y., et al., 2005. Human adipose tissue-derived stem cells differentiate into endothelial cells *in vitro* and improve postnatal neovascularization *in vivo*. *Biochem. Biophys. Res. Commun.* 332 (2), 370–379.
- Chandra, V., et al., 2011. Islet-like cell aggregates generated from human adipose tissue derived stem cells ameliorate experimental diabetes in mice. *PLoS One* 6 (6), e20615.
- Chandra, V., et al., 2009. Generation of pancreatic hormone-expressing islet-like cell aggregates from murine adipose tissue-derived stem cells. *Stem Cells* 27 (8), 1941–1953.
- Chang, J.C., et al., 2011. Primary adipose-derived stem cells enriched by growth factor treatment improves cell adaptability toward cardiovascular differentiation in a rodent model of acute myocardial infarction. *J. Stem Cells* 6 (1), 21–37.
- Crisan, M., et al., 2008. A perivascular origin for mesenchymal stem cells in multiple human organs. *Cell Stem Cell* 3 (3), 301–313.
- Da Silva Meirelles, L., et al., 2006. Mesenchymal stem cells reside in virtually all post-natal organs and tissues. *J. Cell Sci* 119 (Pt 11), 2204–2213.
- De Bari, C., et al., 2001. Multipotent mesenchymal stem cells from adult human synovial membrane. *Arthritis Rheum* 44 (8), 1928–1942.

- De Francesco, F., et al., 2009. Human CD34/CD90 ASCs are capable of growing as sphere clusters, producing high levels of VEGF and forming capillaries. *PLoS One* 4 (8), e6537.
- De Ugarte, D.A., et al., 2003. Comparison of multi-lineage cells from human adipose tissue and bone marrow. *Cells Tissues Organs* 174 (3), 101–109.
- Dominici, M., et al., 2006. Minimal criteria for defining multipotent mesenchymal stromal cells. The International Society for Cellular Therapy position statement. *Cytotherapy* 8 (4), 315–317.
- Ellison, G.M., et al., 2013. Adult c-kit (pos) cardiac stem cells are necessary and sufficient for functional cardiac regeneration and repair. *Cell* 154 (4), 827–842.
- Fang, S., et al., 2012. Generation of functional blood vessels from a single c-kit+ adult vascular endothelial stem cell. *PLoS Biol* 10, e1001407.
- Gaustad, K.G., et al., 2004. Differentiation of human adipose tissue stem cells using extracts of rat cardiomyocytes. *Biochem. Biophys. Res. Commun* 314 (2), 420–427.
- Gentile, P., et al., 2012. A comparative translational study: the combined use of enhanced stromal vascular fraction and platelet-rich plasma improves fat grafting maintenance in breast reconstruction. *Stem Cells Transl. Med* 1 (4), 341–351.
- Gerlach, J.C., et al., 2012. Perivascular mesenchymal progenitors in human fetal and adult liver. *Stem Cells Dev* 21 (18), 3258–3269.
- Gimble, J., Guilak, F., 2003. Adipose-derived adult stem cells: isolation, characterization, and differentiation potential. *Cytotherapy* 5 (5), 362–369.
- Gronthos, S., et al., 2001. Surface protein characterization of human adipose tissue-derived stromal cells. *J. Cell. Physiol* 189 (1), 54–63.
- Gupta, R., et al., 2012. Zfp423 expression identifies committed preadipocytes and localizes to adipose endothelial and perivascular cells. *Cell Metab* 15, 230–239.
- Han, J., et al., 2010. Adipose tissue is an extramedullary reservoir for functional hematopoietic stem and progenitor cells. *Blood* 115 (5), 957–964.
- Hauener, H., et al., 1987. Adipose tissue development: the role of precursor cells and adipogenic factors. Part I: Adipose tissue development and the role of precursor cells. *Klin Wochenschr* 65 (17), 803–811.
- Hong, K.M., et al., 2005. Characterization of human fibrocytes as circulating adipocyte progenitors and the formation of human adipose tissue in SCID mice. *FASEB J* 19 (14), 2029–2031.
- Im, G.I., et al., 2005. Do adipose tissue-derived mesenchymal stem cells have the same osteogenic and chondrogenic potential as bone marrow-derived cells? *Osteoarthritis Cartilage* 13, 845–853.
- Jankowski, R.J., et al., 2002. The role of CD34 expression and cellular fusion in the regeneration capacity of myogenic progenitor cells. *J. Cell Sci* 115 (Pt 22), 4361–4374.
- Jeon, B.G., et al., 2011. Characterization and comparison of telomere length, telomerase and reverse transcriptase activity and gene expression in human mesenchymal stem cells and cancer cells of various origins. *Cell Tissue Res* 345 (1), 149–161.
- Jiang, Y., et al., 2002. Multipotent progenitor cells can be isolated from postnatal murine bone marrow, muscle, and brain. *Exp. Hematol* 30 (8), 896–904.
- Kajiyama, H., et al., 2010. Pdx1-transfected adipose tissue-derived stem cells differentiate into insulin-producing cells in vivo and reduce hyperglycemia in diabetic mice. *Int. J. Dev. Biol* 54 (4), 699–705.
- Katz, A.J., et al., 1999. Emerging approaches to the tissue engineering of fat. *Clin Plast Surg* 26 (4), 587–603, viii.
- Kim, S.W., et al., 2012. Mesenchymal stem cells overexpressing GCP-2 improve heart function through enhanced angiogenic properties in a myocardial infarction model. *Cardiovasc. Res* 95 (4), 495–506.
- Kinnaird, T., et al., 2004. Marrow-derived stromal cells express genes encoding a broad spectrum of arteriogenic cytokines and promote in vitro and in vivo arteriogenesis through paracrine mechanisms. *Circ. Res* 94 (5), 678–685.
- Ko, M.S., et al., 2011. Effects of expanded human adipose tissue-derived mesenchymal stem cells on the viability of cryopreserved fat grafts in the nude mouse. *Int. J. Med. Sci* 8 (3), 231–238.
- Kucia, M., et al., 2006. A population of very small embryonic-like (VSEL) CXCR4(+) SSEA-1(+)Oct-4+ stem cells identified in adult bone marrow. *Leukemia* 20 (5), 857–869.
- Lee, S.K., et al., 2012. Facial soft tissue augmentation using autologous fat mixed with stromal vascular fraction. *Arch. Plast. Surg* 39 (5), 534–539.
- Lee, R.H., et al., 2004. Characterization and expression analysis of mesenchymal stem cells from human bone marrow and adipose tissue. *Cell. Physiol. Biochem* 14 (4–6), 311–324.
- Li, T.S., et al., 2012. Direct comparison of different stem cell types and subpopulations reveals superior paracrine potency and myocardial repair efficacy with cardiosphere-derived cells. *J. Am. Coll. Cardiol.* 59 (10), 942–953.
- Lin, C.S., et al., 2010. Defining adipose tissue-derived stem cells in tissue and in culture. *Histol. Histopathol* 25 (6), 807–815.
- Lin, G., et al., 2009. Treatment of type 1 diabetes with adipose tissue-derived stem cells expressing pancreatic duodenal homeobox 1. *Stem Cells Dev* 18 (10), 1399–1406.
- Lin, T.M., et al., 2005. Accelerated growth and prolonged lifespan of adipose tissue-derived human mesenchymal stem cells in a medium using reduced calcium and antioxidants. *Stem Cells Dev* 14 (1), 92–102.
- Madonna, R., et al., 2008. Myocardin a enhances telomerase activities in adipose tissue mesenchymal cells and embryonic stem cells undergoing cardiovascular myogenic differentiation. *Stem Cells* 26 (1), 202–211.
- Mangi, A.A., et al., 2003. Mesenchymal stem cells modified with Akt prevent remodeling and restore performance of infarcted hearts. *Nat. Med* 9 (9), 1195–1201.
- Meeran, S.M., et al., 2010. Sulforaphane causes epigenetic repression of hTERT expression in human breast cancer cell lines. *PLoS One* 5 (7), e11457.
- Menasché, P., 2005. Stem cells for clinical use in cardiovascular medicine: current limitations and future perspectives. *Thromb. Haemostasis* 94 (4), 697–701.
- Metzele, R., et al., 2011. Human adipose tissue-derived stem cells exhibit proliferation potential and spontaneous rhythmic contraction after fusion with neonatal rat cardiomyocytes. *FASEB J* 25 (3), 830–839.
- Mizuno, H., et al., 2002. Myogenic differentiation by human processed lipoaspirate cells. *Plast. Reconstr. Surg* 109, 199–209.
- Miura, M., et al., 2003. SHED: stem cells from human exfoliated deciduous teeth. *Proc. Nat. Acad. Sci. U.S.A* 100 (10), 5807–5812.
- Murry, C.E., et al., 2004. Haematopoietic stem cells do not transdifferentiate into cardiac myocytes in myocardial infarcts. *Nature* 428 (6983), 664–668.
- Ning, H., et al., 2006. Neuron-like differentiation of adipose tissue-derived stromal cells and vascular smooth muscle cells. *Differentiation* 74 (9–10), 510–518.
- Noort, W.A., et al., 2002. Mesenchymal stem cells promote engraftment of human umbilical cord blood-derived CD34(+) cells in NOD/SCID mice. *Exp. Hematol* 30 (8), 870–878.
- Nöth, U., et al., 2002. Multilineage mesenchymal differentiation potential of human trabecular bone-derived cells. *J. Orthop. Res* 20 (5), 1060–1069.
- Ogawa, R., et al., 2004. Osteogenic and chondrogenic differentiation by adipose-derived stem cells harvested from GFP transgenic mice. *Biochem. Biophys. Res. Commun* 313 (4), 871–877.
- Park, E., Patel, A.N., 2010. Changes in the expression pattern of mesenchymal and pluripotent markers in human adipose-derived stem cells. *Cell Biol. Int* 34 (10), 979–984.
- Paul, A., et al., 2012. PAMAM dendrimer-baculovirus nanocomplex for microencapsulated adipose stem cell-gene therapy: in vitro and in vivo functional assessment. *Mol. Pharmacol* 9 (9), 2479–2488.
- Pérez-Cano, R., et al., 2012. Prospective trial of adipose-derived regenerative cell (ADRC)-enriched fat grafting for partial mastectomy defects: the RESTORE-2 trial. *Eur. J. Surg. Oncol* 38 (5), 382–389.
- Prunet-Marcassus, B., et al., 2006. From heterogeneity to plasticity in adipose tissues: site-specific differences. *Exp. Cell Res* 312 (6), 727–736.
- Quirici, N., et al., 2010. Anti-L-NGFR and -CD34 monoclonal antibodies identify multipotent mesenchymal stem cells in human adipose tissue. *Stem Cells Dev* 19 (6), 915–925.
- Rada, T., et al., 2011. Distinct stem cells subpopulations isolated from human adipose tissue exhibit different chondrogenic and osteogenic differentiation potential. *Stem Cell Rev* 7 (1), 64–76.
- Rodeheffer, M.S., et al., 2008. Identification of white adipocyte progenitor cells in vivo. *Cell* 135 (2), 240–249.
- Ryu, Y.J., et al., 2013. Phenotypic characterization and in vivo localization of human adipose-derived mesenchymal stem cells. *Mol. Cell* 35 (6), 557–564.
- Sachs, P.C., et al., 2012. Defining essential stem cell characteristics in adipose-derived stromal cells extracted from distinct anatomical sites. *Cell Tissue Res* 349, 505–515.
- Sakaguchi, Y., et al., 2005. Comparison of human stem cells derived from various mesenchymal tissues: superiority of synovium as a cell source. *Arthritis Rheum* 52 (8), 2521–2529.
- Sampaolei, M., et al., 2003. Cell therapy of alpha-sarcoglycan null dystrophic mice through intra-arterial delivery of mesoangioblasts. *Science* 301 (5632), 487–492.
- Schäffler, A., et al., 2007. Concise review: adipose tissue-derived stromal cells—basic and clinical implications for novel cell-based therapies. *Stem Cells* 25 (4), 818–827.
- Scholz, T., et al., 2009. Correlation of rapid phenotypic changes and insulin production of differentiated human adipose tissue-derived stem cells. *Ann. Plast. Surg* 63 (4), 436–440.
- Sen, A., et al., 2001. Adipogenic potential of human adipose derived stromal cells from multiple donors is heterogeneous. *J. Cell. Biochem* 81 (2), 312–319.
- Sengenès, C., et al., 2007. Chemotaxis and differentiation of human adipose tissue CD34+/CD31– progenitor cells: role of stromal derived factor-1 released by adipose tissue capillary endothelial cells. *Stem Cells* 25 (9), 2269–2276.
- Sengenès, C., et al., 2005. Preadipocytes in the human subcutaneous adipose tissue display distinct features from the adult mesenchymal and hematopoietic stem cells. *J. Cell. Physiol* 205 (1), 114–122.
- Seo, M.J., et al., 2005. Differentiation of human adipose stromal cells into hepatic lineage in vitro and in vivo. *Biochem. Biophys. Res. Commun* 328 (1), 258–264.
- Shen, C., et al., 2009. The detection of circulating tumor cells of breast cancer patients by using multimarker (Survivin, hTERT and hMAM) quantitative real-time PCR. *Clin Biochem* 42 (3), 194–200.
- Timper, K., et al., 2006. Human adipose tissue-derived mesenchymal stem cells differentiate into insulin, somatostatin, and glucagon expressing cells. *Biochem. Biophys. Res. Commun.* 341 (4), 1135–1140.
- Toma, J.G., et al., 2005. Isolation and characterization of multipotent skin-derived precursors from human skin. *Stem Cells* 23 (6), 727–737.
- Traktuev, D.O., et al., 2008. A population of multipotent CD34-positive adipose stromal cells share pericyte and mesenchymal surface markers, reside in a periendothelial location, and stabilize endothelial networks. *Circ. Res* 102 (1), 77–85.
- Tran, K.-V., et al., 2012. The vascular endothelium of the adipose tissue gives rise to both white and brown fat cells. *Cell Metab* 15, 222–229.
- Tuli, R., et al., 2003. A simple, high-yield method for obtaining multipotential mesenchymal progenitor cells from trabecular bone. *Mol. Biotechnol* 23 (1), 37–49.

- Varma, M.J.O., et al., 2007. Phenotypical and functional characterization of freshly isolated adipose tissue-derived stem cells. *Stem Cells Dev* 16 (1), 91–104.
- Wan Safwani, W.K., et al., 2011. The changes of stemness biomarkers expression in human adipose-derived stem cells during long-term manipulation. *Biotechnol. Appl. Biochem* 58 (4), 261–270.
- Wang, Y., et al., 2012. Adipose derived mesenchymal stem cells transplantation via portal vein improves microcirculation and ameliorates liver fibrosis induced by CCl4 in rats. *J. Transl. Med* 10, 133.
- Wosnitza, M., et al., 2007. Plasticity of human adipose stem cells to perform adipogenic and endothelial differentiation. *Differentiation* 75 (1), 12–23.
- Yoshimura, K., et al., 2010. Progenitor-enriched adipose tissue transplantation as rescue for breast implant complications. *Breast J* 16 (2), 169–175.
- Yoshimura, K., et al., 2008a. Cell-assisted lipotransfer for cosmetic breast augmentation: supportive use of adipose-derived stem/stromal cells. *Aesthetic Plast. Surg* 32 (1), 48–55.
- Yoshimura, K., et al., 2008b. Cell-assisted lipotransfer for facial lipoatrophy: efficacy of clinical use of adipose-derived stem cells. *Dermatol. Surg* 34 (9), 1178–1185.
- Yoshimura, K., et al., 2006. Characterization of freshly isolated and cultured cells derived from the fatty and fluid portions of liposuction aspirates. *J. Cell. Physiol* 208 (1), 64–76.
- Young, H.E., Black, A.C., 2004. Adult stem cells. *Anat. Rec. Part A: Discoveries Mol. Cell. Evol. Biol* 276 (1), 75–102.
- Young, H.E., et al., 2004. Adult reserve stem cells and their potential for tissue engineering. *Cell Biochem. Biophys* 40 (1), 1–80.
- Zamperone, A., et al., 2013. Isolation and characterization of a spontaneously immortalized multipotent mesenchymal cell line derived from mouse subcutaneous adipose tissue. *Stem Cells Dev* 22 (21), 2873–2884.
- Zannettino, A.C., et al., 2007. Human multipotential mesenchymal/stromal stem cells are derived from a discrete subpopulation of STRO-1^{bright}/CD34⁺/CD45⁽⁻⁾/glycophorin-A⁻ bone marrow cells. *Haematologica* 92 (12), 1707–1708.
- Zuk, P.A., et al., 2001. Multilineage cells from human adipose tissue: implications for cell-based therapies. *Tissue Eng* 7 (2), 211–228.